A Spectral Technique for Estimating Turbulent Stress, Scalar Flux Magnitude, and Eddy Viscosity in the Ocean Boundary Layer under Pack Ice

Miles G. McPhee

McPhee Research Company, Naches, Washington

ABSTRACT

The hypothesis is tested that, for the planetary boundary layer, turbulent vertical velocity (w) spectral density, normalized by u_*^2/k (u_*^2 is Reynolds stress magnitude and k is wavenumber: 2π times frequency divided by mean flow speed), is a "universal" function of nondimensional wavenumber k/k_{max}, where k_{max} is the wavenumber at the peak in the area-preserving log–log w spectrum. Data from clusters of turbulence-measuring instruments deployed through the ocean boundary layer beneath pack ice during the yearlong Surface Heat Budget of the Arctic (SHEBA) project were analyzed by averaging spectra in 3-h bins, then nondimensionalizing weighted w spectral density by directly measured Reynolds stress magnitude and wavenumber by k_{max}. In the outer boundary layer, normalized spectra were remarkably uniform, suggesting that (i) the fundamental turbulence scale is inversely proportional to k_{max} and (ii) the w wavenumber spectrum by itself may be used to estimate local stress magnitude and eddy viscosity. The arguments are extended to a scalar variable (temperature) using a combination of the w and scalar spectra, in a way somewhat analogous to the inertial dissipation method used for the atmospheric surface layer. Spectral estimates of turbulent heat flux agreed reasonably well with direct covariance estimates. The structure of the vertical velocity spectrum in the outer boundary layer implies that, in a neutrally stratified, homogeneous flow, production of turbulent kinetic energy (TKE) exceeds dissipation by a significant factor, with the balance provided mainly by vertical TKE turbulent flux divergence.

1. Introduction

In a summary of turbulent velocity spectra measured in the lower part of the atmospheric boundary layer, Busch and Panofsky (1968) noted that (i) wavelengths at the maximum in the logarithmic spectra of vertical velocity increased linearly with height up to about 50 m (the atmospheric surface layer), and more slowly thereafter; (ii) nondimensional frequency, $f_m = nz/V$ (where n is frequency and V is mean wind velocity) at the spectral maximum scaled with Monin–Obukhov similarity in the surface layer; (iii) there was a relatively uniform ("universal") shape to the nondimensionalized w spectra, when abscissa values were scaled by f_m and ordinate values by u_{*0}^2, the kinematic surface stress magnitude; and (iv) the *alongstream* (longitudinal) spectra did not exhibit correspondingly predictable behavior. An immediate consequence is that for the neutrally stratified atmospheric surface layer, the wavenumber ($k_{max} = f_m/z$) at the spectral maximum varies inversely as distance from the surface. In the neutral surface layer, mixing length, $\lambda = K_m/u_{*0} = \kappa z$ (where κ is von Kármán's constant and K_m is eddy viscosity), is thus inversely proportional to k_{max}. Busch and Panofsky surmised that

the connection between λ and k_{max} might persist beyond the surface layer where λ loses its z dependence.

In the ocean boundary layer (OBL), the region where distance from the boundary determines the size of energy containing turbulent eddies (the *surface layer* in atmospheric terminology) extends at most only a few meters. Vertical turbulent velocity spectra from eight levels spanning the entire OBL ($\sim$35 m) under drifting sea ice, reported by McPhee and Smith (1976), confirmed that k_{max} did not scale with $1/z$ beyond about 4 m from the ice–water interface. We adapted the idea of an inverse relationship between λ and k_{max} to estimate nondimensional eddy viscosity at specific levels, which compared favorably with results from numerical boundary layer models at the time. These and later observations (McPhee and Martinson 1994; McPhee 1994; McPhee and Stanton 1996) suggested that, for the entire boundary layer, mixing length was better described as proportional to $1/k_{max}$ rather than distance from the boundary. Basing eddy viscosity and diffusivity on the product of the local friction velocity, $u_* = (\langle u'w'\rangle^2 + \langle v'w'\rangle^2)^{1/4}$, and $\lambda = c_\lambda/k_{max}$ described measurements from the outer part of the boundary layer quite well. In what follows, the convention is adopted that *surface layer* refers to that part of the OBL where mixing length varies with $|z|$, vis-a-vis the *outer layer,* where z dependence is negligible.

Corresponding author address: Dr. Miles G. McPhee, McPhee Research Company, 450 Clover Springs Road, Naches, WA 98937. E-mail: mmcphee@starband.net

The yearlong dataset of turbulence measurements made at several levels in the OBL under drifting pack ice in the Arctic Ocean during the Surface Heat Budget of the Arctic (SHEBA) project provides a unique opportunity to test relationships between turbulence spectra (velocity and scalar) and measured fluxes of momentum and heat. Uttal et al. (2002) present an overview of the SHEBA project, in which an icebreaker drifted passively with the ice in the western Arctic Ocean from October 1997 through September 1998. An inverted mast with turbulence instrument clusters (TICs) under the multiyear SHEBA ice floe provided turbulence measurements at nominal levels 4, 8, 12, and 16 m below the ice undersurface for the first half of the project, and at two levels for the remainder. Each instrument cluster comprised three small, partially ducted mechanical current meters, mounted along mutually orthogonal axes, near fast-response thermometers (Sea-Bird Electronics, SBE 03) and ducted conductivity sensors (SBE 04). One cluster included an open electrode microstructure conductivity sensor (SBE 07). Further details of the ocean turbulence deployment and data processing are given by McPhee (2002). About half way through the experiment, ice deformation forced abandonment of the initial station (site 1) set up adjacent to the ship. The ocean measuring program was relocated to a different part of the floe (site 2), where it remained for the rest of the experiment. At site 2 during July 1998 biofouling sometimes degraded the data, which were not used here. The mechanical current-meter triads do not adequately measure three-dimensional flow at mean current speeds less than about 0.05 m s^{-1}, but throughout the project ice speed was typically 2% of the near-surface wind speed, so this was a limitation only during exceptionally calm periods.

The TIC system is capable of measuring all three velocity components along with temperature well into the inertial subrange of the turbulent kinetic energy (TKE) spectrum. Vertical turbulent fluxes of momentum and sensible heat were estimated by calculating the covariance of vertical velocity with horizontal velocity deviations and temperature deviations, respectively, over 15-min realizations of the flow field (typically representing a spatial displacement of 100–200 m).[1] Variance spectra for the individual velocity components and deviatory temperature were also calculated. The 15-min realizations were then further averaged in 3-h bins (except as noted below).

An established tradition exists for using spectral densities in the inertial subrange of turbulent velocity and scalar spectra to estimate turbulent fluxes (e.g., Kol-

mogorov 1941; Hinze 1975; Edson et al. 1991). Using, for example, friction velocity (momentum flux), the usual approach is to simplify the steady, horizontally homogeneous TKE equation

$$P_s + P_b = D + \varepsilon \qquad (1)$$

to a balance between production by shear ($P_s = \boldsymbol{\tau} \cdot \mathbf{U}_z$, where $\boldsymbol{\tau}$ is kinematic Reynolds stress and $\mathbf{U}_z$ is velocity shear) and by buoyancy ($P_b = -\langle w'b' \rangle$, i.e., the negative of turbulent buoyancy flux) versus dissipation at molecular scales (ε). Term D, the vertical divergence of TKE flux and pressure velocity covariance, is usually neglected. For near-neutral stability in the atmospheric surface layer, the balance is simply expressed as $u_{*0} = (\varepsilon \kappa z)^{1/3}$, which follows from $u_{*0}^2 = \kappa u_{*0} z U_z$. Dissipation is obtained from the spectral density of, say, alongstream velocity (S_{uu}) evaluated at a wavenumber within the inertial subrange:

$$S_{uu}(k) = \alpha_\varepsilon \varepsilon^{2/3} k^{-5/3}, \qquad (2)$$

where α_ε is the Kolmogorov constant. Similar reasoning provides estimates of scalar flux magnitude by equating the production of, for example, thermal variance to thermal dissipation and using thermal spectral density in the inertial subrange in combination with ε to calculate thermal dissipation, whence the magnitude of scalar flux $|\langle w'T \rangle|$. Here again thermal flux and mean gradient are related by eddy diffusivity, assumed proportional to κz (modified by Monin–Obukhov stability functions) in the surface layer. The approach is commonly referred to as the inertial dissipation method (Edson et al. 1991).

For the outer layer, a drawback of the inertial dissipation method (apart from the issue of λ losing its z dependence) is the difficulty in confirming a crucial assumption of the technique, namely, that the vertical transport term D in (1) is negligible. Shear production falls rapidly with distance from the boundary; thus, even if the neglected turbulent transport term is only a small fraction of shear production near the surface, it can be a significant factor in the outer layer. Using the square root of the density ratio as a scaling factor, the standard 10-m measurement height in the atmosphere corresponds to about 1/3 m in the OBL, with a neutral mixing length there of 0.13 m. In the outer layer, typical values of λ for the under-ice OBL are about 2 m (e.g., McPhee and Martinson 1994). For concreteness, suppose measurements made 1/3 m from horizontally uniform ice in a steady, neutral flow indicated a dissipation rate $\varepsilon = 7 \times 10^{-6}$ W kg^{-1} (a typical value) and that in actuality production exceeded dissipation by 5% (i.e., $D = 3.5 \times 10^{-7}$ W kg^{-1}). Assuming a balance between production and dissipation would underestimate $u_* = (\varepsilon \lambda)^{1/3}$ by about 2%. Now suppose further that friction velocity and TKE transport at 3.5 m (near the far extent of the surface layer, with $\lambda = 1.4$ m) were comparable to values near the surface. Then $P_s = u_*^3/\lambda \sim 7 \times 10^{-7}$ W kg^{-1}, about 2 times the dissipation rate, and now assuming a balance

---

[1] In principle, the TICs also furnish estimates of salinity flux, and, indeed, the cluster equipped with a microstructure conductivity meter at times provided robust estimates of $\langle w'S' \rangle$; however, the sensors are fickle and the salinity flux data and its relation to covariance calculated with the ducted conductivity meters will be treated elsewhere.

between production and dissipation would underestimate u_* by about 20%.

This paper departs from previous treatment of the modified inertial dissipation technique (e.g., McPhee 1994) by retreating to a naïve view in which straightforward dimensional analysis (e.g., Barenblatt 1996) is used to relate variance spectra of vertical velocity and deviatory temperature to measured fluxes. This obviates the need for external specification of the Kolmogorov constants as in (2). The approach here is phenomenological in that scales are chosen from dimensional analysis, assuming that the w spectrum is governed over some chosen wavenumber range by a strictly limited number of variables, including a length scale inversely proportional to k_{max}. The choice of scales is tested by examining how well the scaled spectra conform to a "universal" shape.

Section 2 is about calculating local friction speed directly from the w spectrum. Section 3 extends the technique to estimate turbulent heat flux magnitude from the temperature variance spectrum. In section 4, estimates of TKE production and dissipation are compared. Results are summarized in section 5.

2. Estimating u_* from the w spectrum

A direct approach to estimating momentum flux magnitude from the vertical velocity spectrum is as follows. Suppose that the fundamental turbulent length scale (mixing length) is inversely proportional to k_{max} and that buoyancy forces in the fluid are negligible as compared with inertial forces (the usual situation in the OBL under thick ice away from the ice margins). Postulate that, for near-neutral stability, the weighted spectral energy density [$\phi = kS_{ww}(k)$] depends mainly on the local stress magnitude u_*^2, wavenumber k, and a length scale characterizing the dominant eddies in the flow, $\lambda_{max} = c_\lambda / k_{max}$. Straightforward dimensional analysis then suggests a dimensionless relation of the form

$$\frac{\phi}{u_*^2} = \Phi\left(\frac{k}{k_{max}}\right).$$

The argument depends on buoyancy flux being unimportant in the energy balance. Although rare during the SHEBA project, there were instances during summer when stabilizing buoyancy flux from surface melting appeared to quantitatively impact the boundary layer (McPhee 2002); hence, in the remainder of this section, only data from site 1 (November–March) were used. While the ice continued to grow for most of the winter, the associated destabilizing buoyancy flux was almost always small compared with shear production. There were times, however, when the lowest cluster (TIC 4, nominally 16 m from the ice) was beyond what would be considered the well-mixed layer. Samples for which its salinity differed from TIC 3 (12 m) by more than 0.003 psu were excluded from the analysis here in order
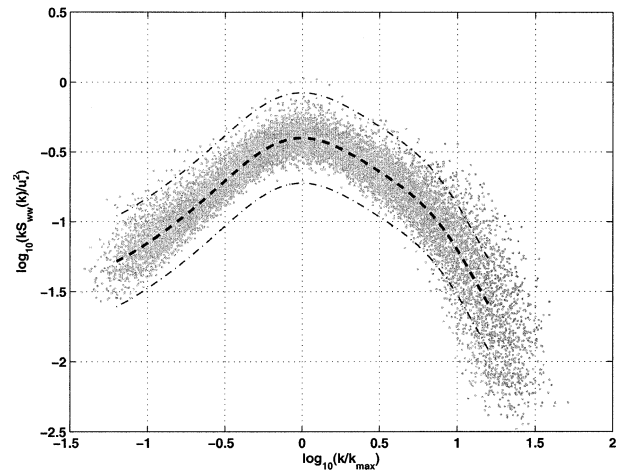

FIG. 1. Vertical velocity spectra from 387 three-hour averages at SHEBA site 1, cluster 2, each normalized by k_{max} (abscissa) and u_*^2/k (ordinate). The thick dashed line is a high-order polynomial fit, with 95% confidence interval indicated by lighter dashed lines, assuming measurement errors are independent and normally distributed with constant variance. Cluster 2 was nominally 8 m below the ice–ocean interface.

to preserve the assumption of negligible buoyancy impact.[2] Cluster 4 was also affected by a faulty rotor during the last part of the site-1 deployment, considerably reducing the number of samples there as compared with the other three clusters.

As in previous analyses (e.g., McPhee and Martinson 1994; McPhee 1994), wavenumber spectra were calculated for each 15-min realization of the turbulent flow by smoothing the periodogram of each time series formed from the product of the Fourier transform with its complex conjugate. The area-preserving (weighted) spectral components [$fS(f) = kS(k)$] were then bin averaged in equally spaced intervals of log$k$, where $k = 2\pi f/U$ is the angular wavenumber derived from frequency f and mean current speed U by Taylor's hypothesis. These were further averaged in 3-h blocks along with the measured covariances and other quantities as in McPhee (2002).

For each cluster, each of the 3-h average weighted w spectra were fitted with a high-order polynomial in order to identify k_{max} at the peak in the spectrum, which was then used to nondimensionalize the abscissa grid, providing the dimensionless wavenumber γ. Similarly, a dimensionless weighted spectral density, $\Phi = kS_{ww}(k)/u_*^2$, was formed by normalizing with the local Reynolds stress, calculated from the average velocity covariance of all 15-min realizations in the 3-h period. An example for cluster 2 (Fig. 1) illustrates that, although there is

---

[2] Individual TIC conductivity sensors were periodically cross calibrated against the SHEBA SBE9+ profiling instrument, providing an accuracy approaching 0.03 S m^{-1}, hence the limit used here. For a difference in salinity of 0.003 psu between TICs 3 and 4, a typical value for the local Obukhov length in the outer layer was ~20 m, with relatively small but not negligible impact in the TKE balance.
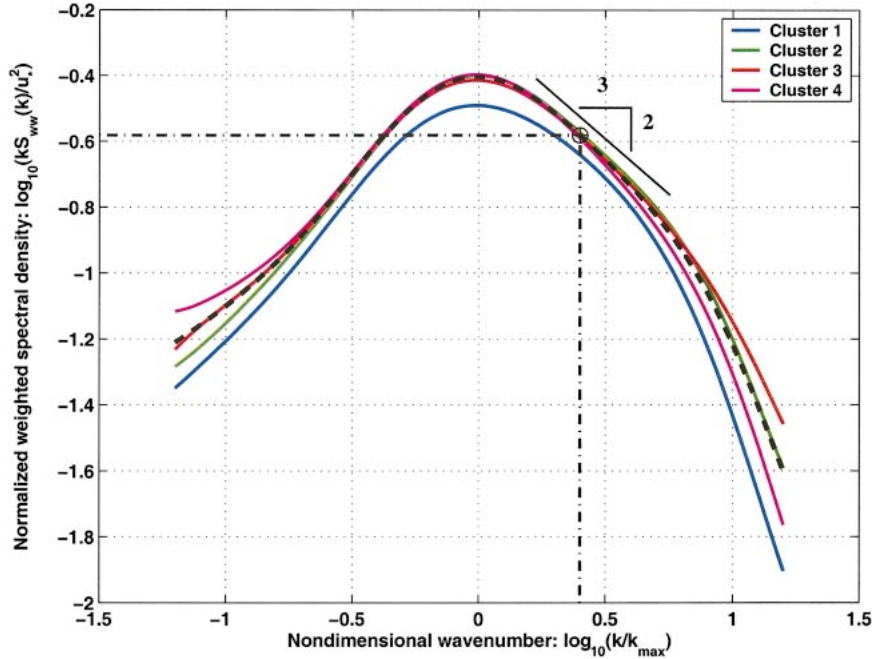
FIG. 2. Polynomial fits to the normalized spectra from all clusters at site 1. Nominal displacements from the ice undersurface are 4, 8, 12, 16 m for TICs 1–4, respectively. The dashed curve is the average fit for TICs 2–4. Dot–dashed vertical and horizontal lines indicate values for γ_* and Φ_*, respectively. The numbers of 3-h samples for TICs 1–4 were 348, 386, 298, and 75, respectively.

fairly large scatter, a common shape emerges to which most of the spectra adhere. A composite normalized spectrum was then formed by a high-order polynomial fit to all of the nondimensional pairs (dashed line in Fig. 1).

The composite spectra for all four clusters deployed during the first half of the experiment (Fig. 2) show a remarkably similar form, especially in the nondimensional wavenumber range $0.3 < \gamma < 3$ for TICs 2–4 (nominally 8–16 m below the ice–ocean interface). TIC 1, nearest the surface, was in the least horizontally homogeneous part of the boundary layer (McPhee 2002). We found in many cases, particularly when the flow (in the measurement reference frame) approached from across a multiyear pressure ridge keel some distance upstream, that turbulent stress and TKE increased with depth from TIC 1 to TIC 2 (4–8 m). From the standpoint of dimensional analysis, this would indicate influence from another independent parameter. The similarity of the composite spectra at the other levels does not preclude influence of this nonhomogeneity factor, but does indicate that its depth dependence must be small in the outer part of the boundary layer. Similar analysis of the alongstream and cross-stream spectra [$kS_{uu}(k)$ and $kS_{vv}(k)$] resulted in much larger scatter in peak values and overall less similarity at the four levels, when nondimensionalized by the inverse wavenumber at the peak of the spectrum and by kinematic stress magnitude (see Fig. 6 below).

Anticipating extension of the spectral technique to scalar variables, we search for a wavenumber subrange in the w spectra, where the TKE transfer to higher wavenumbers depends only on k and the shear production of TKE (assuming negligible buoyancy production)

$$P = |u_*^2 U_z| = \frac{u_*^3}{\lambda} = \frac{u_*^3 k_{max}}{c_\lambda}, \qquad (3)$$

where shear and kinematic stress are related by an eddy viscosity, $K_m = u_*\lambda$. Under these conditions, the weighted spectral density is

$$\phi = f(P, k), \qquad (4)$$

reducing by one the number of independent parameters with independent dimensions, yielding one dimensionless group, and so

$$\phi \propto P^{2/3}k^{-2/3}, \qquad \frac{\phi}{u_*^2} \propto \left(\frac{k}{k_{max}}\right)^{-2/3}, \quad \text{and}$$

$$\Phi = c_\gamma \gamma^{-2/3}. \qquad (5)$$

There is a reasonably well-defined region in the nondimensional spectra where the log–log slope approaches $-2/3$. The symbol with dashed vertical and horizontal lines marks coordinates ($\log\gamma_* = 0.4$; $\log\Phi_* = -0.58$) within this subrange, providing an estimate of the proportionality constant in (5):
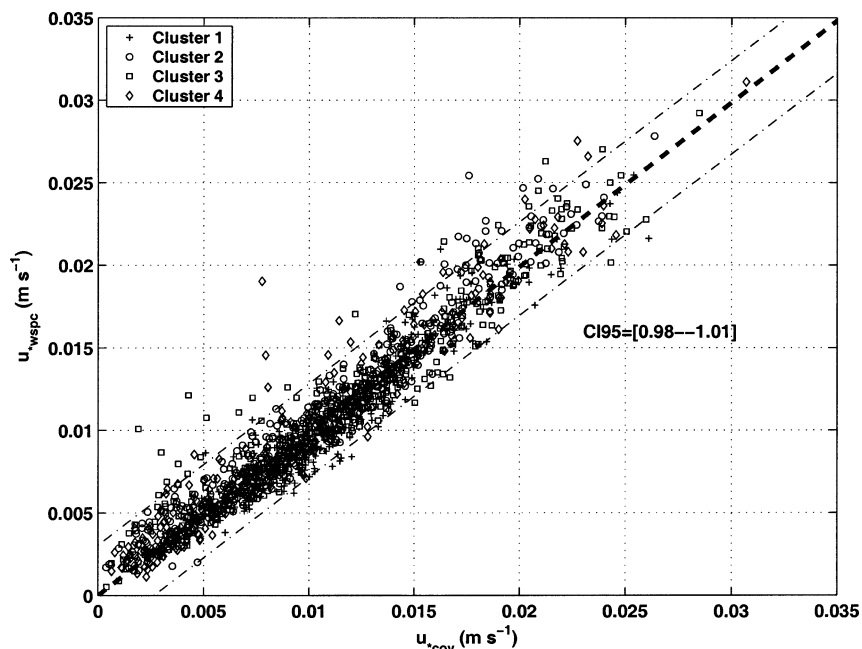
FIG. 3. Scatter diagram of friction velocity calculated from each 3-h sample by the spectral technique (7) vs friction velocity from the square root of measured turbulent Reynolds stress. The thin, dot–dash lines are 95% confidence limits for a linear regression. The heavy dashed line is a least squares fit passing through the origin, with the 95% confidence interval for the slope listed. There are 1549 samples.

$$\log c_\gamma = \log \Phi_* + (2/3) \log \gamma_*. \qquad (6)$$

For the given values, $c_\gamma = 0.48$.

For a particular vertical velocity spectrum, the Reynolds stress magnitude is estimated by (i) determining $\log k_{max}$ by finding the maximum in a polynomial fitted to the bin-averaged log–log spectrum; (ii) evaluating the polynomial at $\log k = \log k_{max} + \log \gamma_*$ to obtain $\log \phi = \log[k S_{ww}(k)]$; and (iii) then calculating u_* according to

$$\log u_* = (1/2)(\log \phi - \log \Phi_*). \qquad (7)$$

Spectral estimates of friction speed are compared with covariance estimates in Fig. 3. A relatively tight relationship is indicated by the small confidence interval for the slope of the linear fit through the origin. Considered individually, only the slope of TIC 1 with a confidence interval of [0.92–0.98] is significantly different from 1. This may be due to horizontal inhomogeneity at that level in the water column, as discussed previously.

3. Spectral estimate of turbulent heat flux magnitude

Heat flux magnitude may also be estimated by combining temperature variance spectra with the spectral estimates of stress. By analogy with the TKE equation, the transfer of thermal variance to higher wavenumbers in an inertial subrange is postulated to depend on ϕ [i.e.,

on shear production of TKE via (3)], on k, and on the production of thermal variance:

$$P_T = \left| \langle w'T' \rangle \frac{dT}{dz} \right| = \frac{\langle w'T' \rangle^2}{\lambda u_*} = \frac{k_{max} \langle w'T' \rangle^2}{c_\lambda u_*}. \qquad (8)$$

By analogous dimensional analysis

$$\phi_T \propto P_T k^{-1} \phi^{-1/2},$$

which combined with (5) and (8) reduces to

$$\phi_T = c_T \gamma_*^{-4/3} \phi^{-1} \langle w'T' \rangle^2,$$

resulting in the nondimensional relation:

$$\frac{\phi_T \phi}{\langle w'T' \rangle^2} = \Phi_{*T},$$

where $\Phi_{*T} = c_T \gamma_*^{-4/3}$. This provides an equation for kinematic heat flux magnitude:

$$\log|\langle w'T' \rangle| = \frac{1}{2}(\log \phi + \log \phi_T - \log \Phi_{*T}); \qquad (9)$$

$\log \phi_T$ is evaluated at $\log k_{max} + \log \gamma_*$.

Regression of spectral estimates versus covariance measurements of turbulent heat flux is shown in Fig. 4. With $c_T = 0.83$, the slope of a least squares fit line through the origin is indistinguishable from unity at the 95% confidence level.

While the scatter in estimates of heat flux magnitude is greater than for friction velocity, the analysis shows
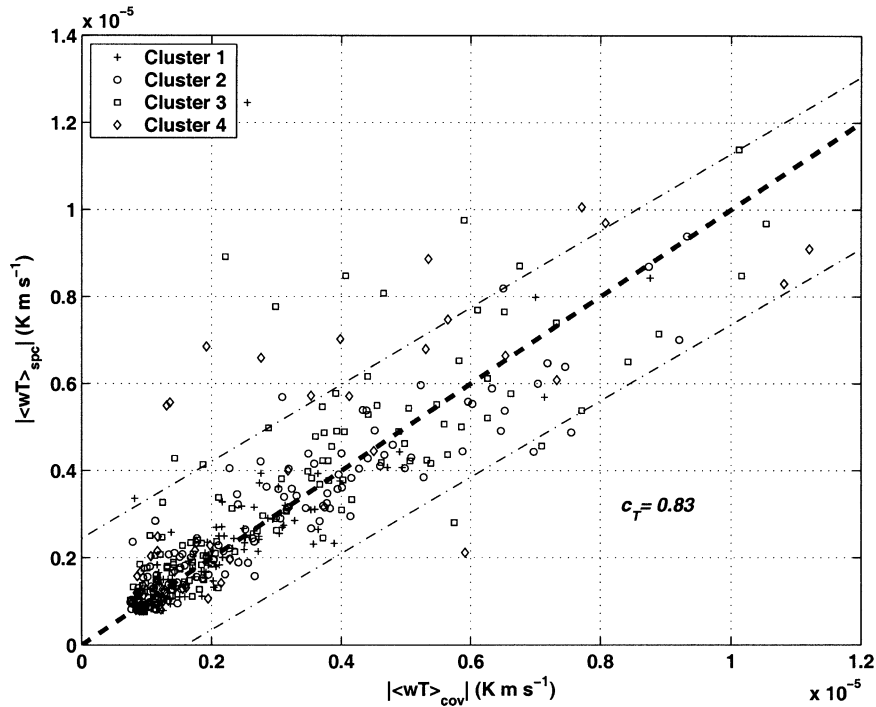
FIG. 4. As in Fig. 3, except showing spectra-derived kinematic heat flux via (9) vs covariance heat flux. There are 396 samples with covariance heat flux magnitude between 3 and 50 W m^{-2}.

that, at least on average, a reasonably good estimate of turbulent heat flux magnitude is possible from temperature and vertical velocity spectra. This is potentially useful in situations where it is impractical to simultaneously deploy three-dimensional current meters and fast-response thermometers capable of measuring the zero-lag covariance directly.

A further demonstration of the spectral technique for estimating momentum and heat flux is provided during a particular storm event near the end of the project, in September 1998. The friction speed and heat flux magnitude calculated from the w and T spectra alone are compared with the corresponding covariance data in Fig. 5. Mean values agree reasonably well and most of the short-term variability is reproduced by the spectral technique. The constants used in the calculation are the same as above, that is, derived during the site-1 drift.

4. Production versus dissipation

Equation (2) provides an estimate of TKE dissipation rate if the cascade of energy through an inertial subrange in the one-dimensional spectrum of alongstream velocity [$\phi_{uu} = kS_{uu}(k)$] is independent of shear (large scales) and viscosity (small scales). If it is further stipulated that turbulence in the inertial subrange is homogeneous and isotropic, there should exist a 4/3 ratio between ϕ_{ww} and ϕ_{uu} in the $-2/3$ log–log range, which is often taken as a test of isotropy (Tennekes and Lumley 1972). If this were the case for the SHEBA neutral data (it is

shown below to be not so), then the ratio of production to dissipation is given by a simple combination of the w spectral parameters:

$$\frac{P_s}{\varepsilon} = \frac{1}{c_\lambda} \left(\frac{4\alpha_\varepsilon}{3c_\gamma} \right)^{3/2}. \tag{10}$$

A commonly accepted value for α_ε is 0.51 (Edson et al. 1991), which combined with $c_\lambda = 0.85$ and $c_\gamma = 0.48$ yields a ratio of about 2, similar to the hypothetical example in section 1.

In order to compare spectra at several levels directly, the dataset was culled to include only times when all four clusters were operating simultaneously, and the stability criterion of section 2 was satisfied. This left a total of 66 three-hour samples, for which composite vertical and alongstream spectra Φ_{ww} and Φ_{uu} were calculated (Fig. 6), where again the abscissa and ordinate were normalized by k_{max} (from the w spectrum) and measured Reynolds stress, respectively. As with the total composite spectra (Fig. 2), Φ_{ww} is remarkably uniform with depth; however, Φ_{uu} varies significantly, with particularly high levels at lower wavenumbers for cluster 2. Most of these data are from relatively early in the project when measured flow approached predominantly from the west across a pressure ridge keel about 110 m upstream from the measurement site. As discussed by McPhee (2002), this had substantial impact on turbulence in the upper part of the boundary layer, including an apparent increase in turbulent stress at midlevels in
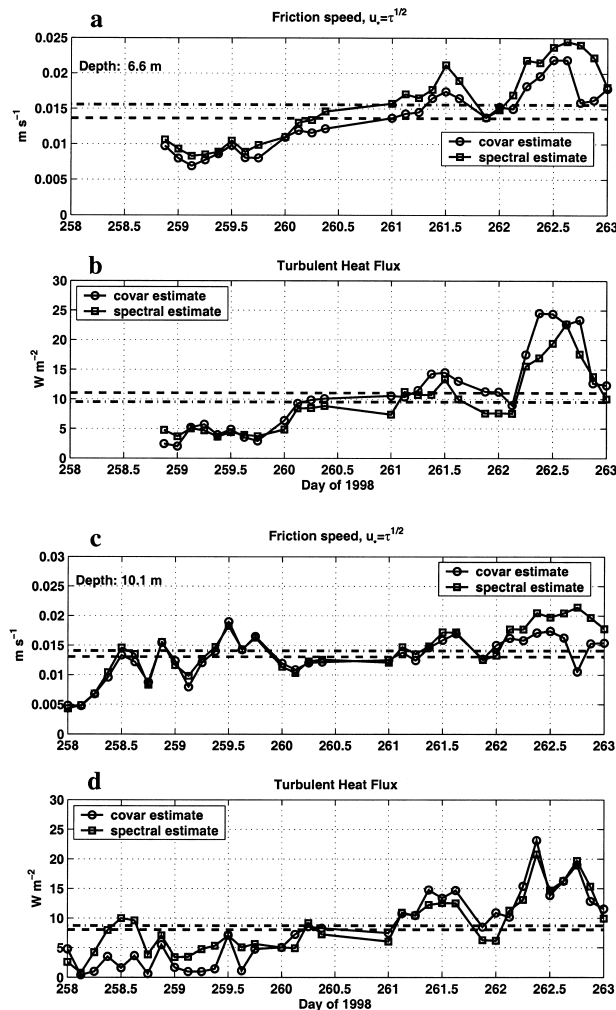
FIG. 5. Comparison of spectra-derived friction velocity and turbulent heat flux with covariance calculations: (a) friction velocity, TIC 1; (b) turbulent heat flux, TIC 1; (c) friction velocity, TIC 2; (d) turbulent heat flux, TIC 2. Dashed lines indicate mean values over the 5-day period for the covariance estimates, and dot–dashed lines are mean values for the spectral estimates. Covariance heat flux is positive upward (toward the ice); spectral estimates provide magnitude only.

the OBL relative to values at 4 m (op. cit., Fig. 5). This behavior is reflected in the alongstream spectra, with the spectral level near the peak in the 8-m spectrum several times that of its 12- and 16-m counterparts. For higher wavenumbers, only for clusters 3 and 4 is $\Phi_{ww} > \Phi_{uu}$, and then not by the separation implied by a 4/3 ratio (0.125 in log–log representation). The implication is that large-scale horizontal heterogeneity in the flow affects the vertical structure of the alongstream (u) spectra much more than it does the w spectra, and must play a significant role in the TKE balance.

With $\alpha_\varepsilon = 0.51$, dissipation was estimated from (2) for each sample in the simultaneous subset for comparison with production from (3), using the covariance estimate of u_* and λ derived from the ϕ_{ww} spectral

peaks. Averaged results from the 66 three-hour samples are summarized in Table 1, which also includes the average of $\langle w'e' \rangle = \langle w'u_i'u_i' \rangle$ (with the summation convention), that is, an estimate of 2 times the vertical turbulent flux of TKE per unit mass. At TICs 1 and 2, dissipation exceeds production, implying for the upper part of the OBL a source of TKE besides local shear. Note that $\langle w'e' \rangle$ at TIC 2 is upward (although small), in contrast to the remaining clusters, supporting the supposition expressed in McPhee (2002) that turbulence near the relatively smooth surface at the measurement site was fed from below by turbulence generated by the prominent topographic feature upstream. At TICs 3 and 4, where the 4/3 isotropy condition is more nearly satisfied, production exceeds dissipation by as much as 76% at 16 m.

The vertical component of the TKE tranport term in (1) is

$$ D = \frac{\partial}{\partial z}\left(\frac{1}{2}\langle w'u_i'u_i' \rangle + \frac{1}{\rho}\langle w'p' \rangle \right), \qquad (11) $$

where the second term on the right is the vertical velocity pressure covariance, not measured by our apparatus. Note that the average imbalance between production and dissipation for TICs 3 and 4 (relatively deep in the OBL) was $P_s - \varepsilon = 0.56 \times 10^{-6}$ W kg^{-1}. If this is representative of the midpoint, a finite-difference approximation of the turbulent TKE flux divergence, that is,

$$ \frac{\partial}{\partial z}\left(\frac{1}{2}\langle w'u_i'u_i' \rangle \right) \approx \frac{(\overline{\langle w'e' \rangle_4} - \overline{\langle w'e' \rangle_3})}{-8} $$

$$ = 0.41 \times 10^{-6} \text{ W kg}^{-1}, $$

accounts (at least in this example) for about 3/4 of the difference.

5. Discussion

The primary result of this paper is that in the near–neutrally stable planetary boundary layer typical of that under drifting sea ice, local Reynolds stress magnitude may be estimated from

$$ u_*^2 = \phi/\Phi_*, $$

where $\phi = kS_{ww}(k)$ evaluated at wavenumber $k = \gamma_* k_{max}$ in the $-2/3$ slope region of the weighted log–log spectrum, and $\Phi_* = c_\gamma \gamma_*^{-2/3}$. The universal constant c_γ was found to be about 0.48, which for the choice of $\gamma_* = 2.51$ yields $\Phi_* = 0.26$. This result does not depend on assuming that TKE production equals dissipation.

For a scalar variable σ, the flux magnitude is given by

$$ |\langle w'\sigma' \rangle| = \left(\frac{\phi\phi_\sigma}{\Phi_{*\sigma}} \right)^{1/2}, \qquad (12) $$

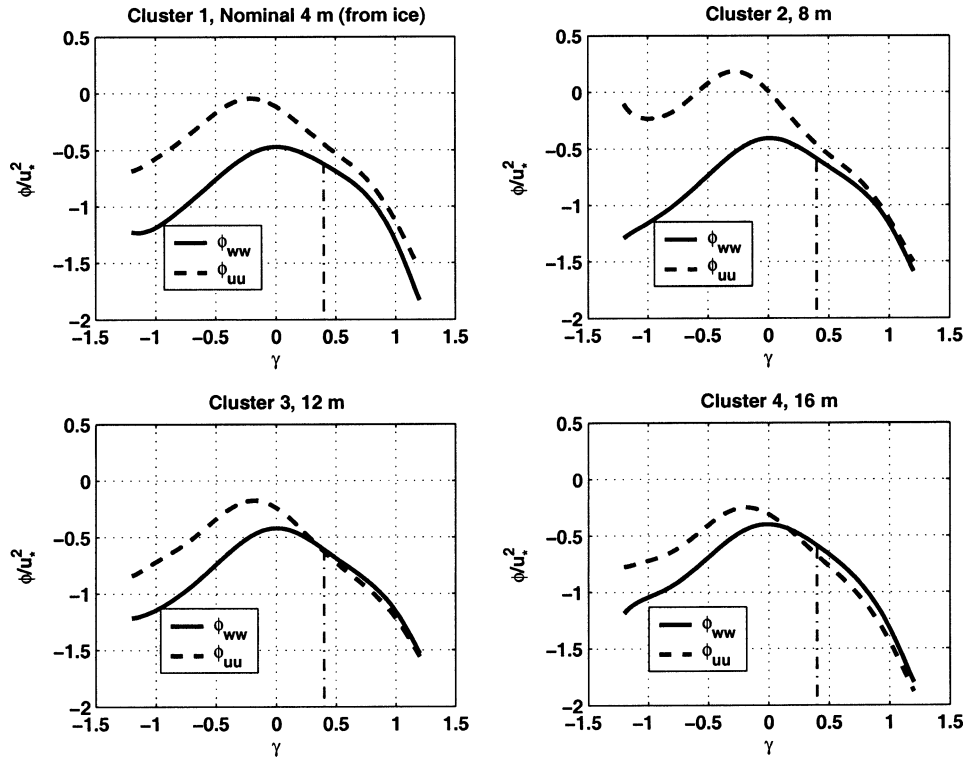where again the weighted spectral densities are evalu-

FIG. 6. Comparison of dimensionless alongstream and vertical velocity spectra, averaged for times when all four TICs were operating simultaneously (66 each, 3-h samples). Abscissas were normalized by k_{max}, evaluated from the peak in the w spectrum in each instance; ordinates were normalized by the measured kinematic Reynolds stress ($\sqrt{\langle u'w'\rangle^2 + \langle u'w'\rangle^2}$). Dot–dashed vertical lines indicate ϕ_{ww} spectral levels in the $-2/3$ region.

ated at $k = \gamma_* k_{max}$. If the Reynolds analogy holds, $\Phi_{*\sigma}$ should apply to all passive tracers. For $\gamma_* = 2.51$, $\Phi_{*T} = 0.24$. If the scalar fluxes are large enough that buoyancy is important in the TKE balance, scales will respond accordingly. Modification for buoyancy is a subject for future work.

Implicit in the spectral approach discussed in section 2 is that kinematic turbulent stress (momentum flux) is proportional to velocity shear: $u_*^2 = K_m U_z$, and that local eddy viscosity is a product of the turbulent velocity scale and the dominant turbulent length scale (McPhee 1994)

$$K_m = u_* \lambda = \frac{u_* c_\lambda}{k_{max}}, \qquad (13)$$

where $c_\lambda \approx 0.85$ is an empirically determined constant.

From a separate line of reasoning, a bulk eddy viscosity may be derived from similarity theory for the neutrally stable boundary layer (McPhee 1981; see also McPhee and Martinson 1994)

$$K_{bulk} = \frac{0.02 u_{*0}^2}{f_{cor}}, \qquad (14)$$

where u_{*0}^2 is kinematic stress at the interface, and f_{cor} is the Coriolis parameter.

For each 3-h segment of data, estimates of interface friction velocity were obtained by adjusting Reynolds stress measurements made at the topmost cluster (TIC 1) to the boundary via the method described by McPhee (2002). At TIC 3 (near the center of the outer OBL), values for local eddy viscosity were calculated from (13)

TABLE 1. Comparison of average turbulence parameters at four levels in the OBL during times when all clusters were operating simultaneously and stratification was negligible (66 three-hour samples); u_* is from the velocity covariance values, and $\lambda = 0.85/k_{max}$.

Cluster	Depth* (m)	u_* (m s^{-1})	λ (m)	P_s (μW kg^{-1})	ε (μW kg^{-1})	P_s/ε	$\langle w'e'\rangle$ (m³ s^{-3})
1	5.8	0.015	2.26	1.49	1.91	0.78	-1.58 ($\times$ 10^{-6} m³ s^{-3})
2	9.8	0.016	2.55	1.60	1.94	0.82	0.63 ($\times$ 10^{-6} m³ s^{-3})
3	13.8	0.017	2.60	1.78	1.19	1.50	-5.29 ($\times$ 10^{-6} m³ s^{-3})
4	17.8	0.016	2.76	1.26	0.72	1.76	-8.61 ($\times$ 10^{-6} m³ s^{-3})

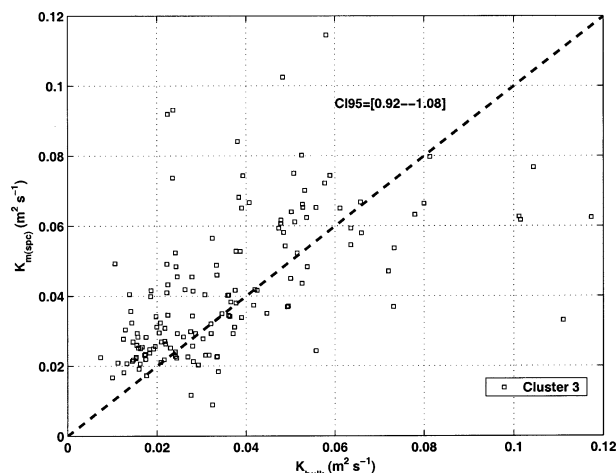* Includes approximately 2.2-m ice draft.

FIG. 7. Scatter diagram of neutrally stable bulk eddy viscosity based on interface friction speed (McPhee and Martinson 1994; McPhee 2002) vs local eddy viscosity at TIC 3 (nominally 12 m from the ice–water interface) calculated exclusively from the vertical velocity spectra. The confidence interval for a least squares fitted straight line through the origin is indicated. There were 148 three-hour samples.

with $c_\lambda = 0.85$ and u_* obtained from (7). The relation between bulk and local eddy viscosity estimates for $u_* > 0.01$ m s^{-1} show much scatter (Fig. 7); nevertheless, a least squares linear fit through the origin has slope 1.00. This correspondence adds additional weight to the idea that it is possible to estimate local eddy viscosity at discrete levels in the OBL solely from information contained in the vertical velocity spectrum.

Besides estimating mixing length and eddy viscosity, the work corroborates earlier findings (McPhee 1994) that it is also possible to make credible estimates of scalar flux magnitude in the outer OBL by combining parameters from the w and scalar spectra.

This analysis affirms that vertical TKE flux divergence is important in the outer OBL. To the extent that the vertical velocity spectra adhere to the nondimen-

sional form of Fig. 2 and that turbulence in the $-2/3$ region of the weighted spectra is isotropic, the vertical transport term in the simplified TKE equation [(1)] should be roughly comparable to dissipation.

REFERENCES

Barenblatt, G. I., 1996: *Scaling, Self-Similarity, and Intermediate Asymptotics.* Cambridge University Press, 386 pp.
Busch, N. E., and H. A. Panofsky, 1968: Recent spectra of atmospheric turbulence. *Quart. J. Roy. Meteor. Soc.,* **94,** 132–147.
Edson, J. B., C. W. Fairall, P. G. Mestayer, and S. E. Larsen, 1991: A study of the inertial-dissipation method for computing air–sea fluxes. *J. Geophys. Res.,* **96,** 10 689–10 711.
Hinze, J. O., 1975: *Turbulence.* 2d ed. McGraw-Hill, 790 pp.
Kolmogorov, A. N., 1941: The local structure of turbulence in incompressible viscous fluid for very large Reynolds number. *Dokl. Akad. Nauk SSSR,* **30,** 299–301.
McPhee, M. G., 1981: An analytic similarity theory for the planetary boundary layer stabilized by surface buoyancy. *Bound.-Layer Meteor.,* **21,** 325–339.
——, 1994: On the turbulent mixing length in the oceanic boundary layer. *J. Phys. Oceanogr.,* **24,** 2014–2031.
——, 2002: Turbulent stress at the ice/ocean interface and bottom surface hydraulic roughness during the SHEBA drift. *J. Geophys. Res.,* **107,** 8037, doi:10.1029/2000JC000633.
——, and J. D. Smith, 1976: Measurements of the turbulent boundary layer under pack ice. *J. Phys. Oceanogr.,* **6,** 696–711.
——, and D. G. Martinson, 1994: Turbulent mixing under drifting pack ice in the Weddell Sea. *Science,* **263,** 218–221.
——, and T. P. Stanton, 1996: Turbulence in the statically unstable oceanic boundary layer under Arctic leads. *J. Geophys. Res.,* **101,** 6409–6428.
Tennekes, H., and J. L. Lumley, 1972: *A First Course in Turbulence.* The MIT Press, 300 pp.
Uttal, T., and Coauthors, 2002: Surface Heat Budget of the Arctic Ocean. *Bull. Amer. Meteor. Soc.,* **83,** 255–275.